Kochi Chapter

Indian Geotechnical Conference
IGC 2022
15th – 17th December, 2022, Kochi

Settlement Based Load-Sharing Ratio Variation for Large Piled-Rafts

Banchiva K. Marak[1] and Baleshwar Singh[2]

[1] Research Scholar, Department of Civil Engineering, IIT Guwahati, Guwahati-781039, Email: k.banchiva@iitg.ac.in
[2] Professor, Department of Civil Engineering, IIT Guwahati, Guwahati-781039, Email: baleshwar@iitg.ac.in

Abstract. In the piled-raft (PR) foundation design, evaluating the load shared between the raft and piles is important as both contribute to the load-carrying capacity. For the present study, three-dimensional numerical modeling has been carried out to investigate the load-sharing ratio of a large piled-raft foundation in dense sand with respect to settlement by varying parameters like spacing and length of pile and thickness of raft. Initially, the individual load-settlement responses of the raft and piles in PR are determined for all PR configurations and then compared with the individual responses of the unpiled raft and group piles. Results show that the load-carrying capacity of raft and piles in PR is found to be greater than unpiled raft and group piles, respectively, for smaller pile spacing. The load-sharing ratio increases with increase of pile spacing at all settlement levels. With increasing settlement, the load-sharing ratio decreases for smaller pile spacing, whereas, for larger pile spacing, it increases initially and then decreases. As pile length increases, the proportion of load carried by piles increases at all settlement levels for smaller pile spacing; but for larger pile spacing, the variation of the proportion of load carried by piles is not significant at smaller settlement levels. For all raft thicknesses at higher pile spacing, the proportion of load carried by piles increases initially at initial settlement and then becomes almost constant towards higher settlement.

Keywords: Large piled-rafts; Dense sand; Load-settlement response; Unpiled raft; Group piles; Load-sharing ratio.

1 Introduction

Piled-raft foundation is a hybrid foundation system that is composed of two structural components that is, the raft and the piles. This foundation system is designed in such a way to utilize the capacity of both the structural components and hence, allow for load sharing between them. This load-sharing mechanism makes this foundation system as the alternative economical option when used in suitable geotechnical conditions, in comparison to the conventional pile foundation in which the capacity of the raft is not taken into consideration. Due to the combined action of both the structural components, the stress as well as displacement fields of the raft and piles overlap, giving rise to various interactions between the raft, piles, and soil, making the overall response of

piled-raft foundation very complex [1]**.** As a result of these interactions, the load-carrying capacity of raft and piles, when combined into piled-raft, becomes different from that of alone unpiled raft (UR) and group piles (GP) [2]. One of the important design components for achieving the optimum piled-rafts is evaluating the load shared between the raft and piles since the contribution of both raft and piles plays an important role in the load-carrying capacity of the piled-raft foundation. This raft and pile load share is generally expressed in terms of load-sharing ratio, defined as the ratio of the proportion of load carried by the piles to the total applied load on piled-raft. The piled-raft foundations are categorized into small piled-rafts and large piled-rafts, according to Viggiani et al. [3]. Small piled-rafts are those in which the width of the raft (B_r) is small as compared to the length of the piles (L) ($B_r/L < 1$), with the width of the raft ranging from 5 m to 15 m. Large piled-rafts are those in which the width of the raft is comparatively large with respect to the length of piles ($B_r/L > 1$), with the width of the raft greater than15 m.

The objective of the present study is to investigate the load-sharing ratio of a large piled-raft foundation in dense sand with respect to average settlement by varying parameters like pile spacing and length and raft thickness. The individual load-settlement responses of the raft and piles in PR are determined initially for all PR configurations, which is then compared with the responses of the unpiled raft and group piles alone.

2 Numerical Modeling

This section discusses the numerical modeling procedure and also the validation study of large PR foundations in dense sand. Three-dimensional numerical modeling is carried out with a finite element-based commercial software Plaxis 3D [4]. A suitable mesh size is considered for the analysis on the basis of a mesh convergence study. The numerical model is verified with the centrifuge test results of Park and Lee [1] by modeling the foundation on a prototype scale.

2.1 Domain Size and Mesh Convergence

The size of the soil model is fixed at a lateral distance of 4.5 times the raft width from the edge of the raft on all four sides restraining the horizontal movement and allowing for vertical movement. The vertical depth of the soil domain is taken as seven times the pile length from the base of the raft and the bottom boundary of the soil is fixed; that is, both vertical and horizontal movements are not allowed. The boundaries of the soil model have been selected, keeping in mind that the piled-raft influence zone is well within the soil domain to avoid any undesirable boundary effects. Fig. 1 shows the numerical model with the selected boundaries used for the study, along with piled-raft geometry.

Mesh convergence analysis is performed to identify the optimal mesh required to perform the numerical analysis accurately by considering the available five different meshing options in the Plaxis library (such as very coarse, coarse, medium, fine, and very fine). Coarser meshes are unable to take into account of the important soil and structure behavioral characteristics, while very fine mesh takes excessive computational time for the analysis. The element size according to different meshes is identified by non-dimensional element length, which is defined as the ratio of the length of the

element to the maximum dimension of the model geometry. The result of the mesh convergence study is shown in Fig. 2. It is found that the load-carrying capacity of piled-raft varies a lot when the mesh is changed from very coarse to fine. However, the results almost converge beyond the fine mesh, and hence, fine meshing is adopted for the present numerical analysis. Meshes are refined locally nearby the structural elements.

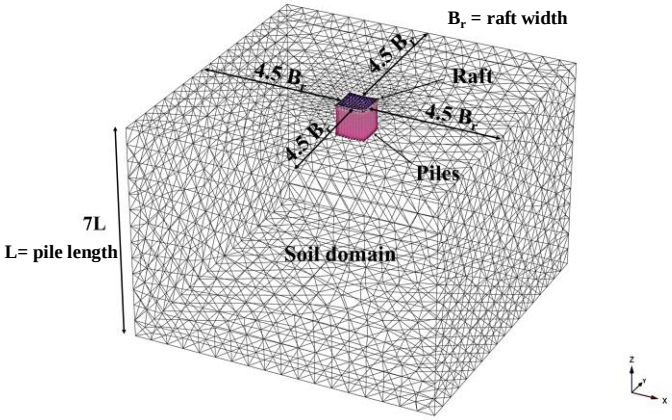

Fig. 1. Numerical model geometry and meshing.

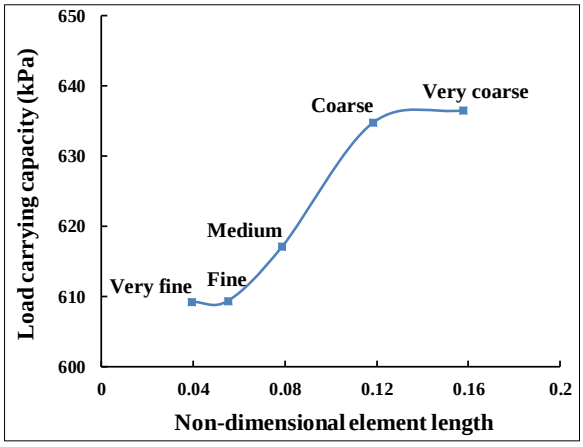

Fig. 2. Mesh convergence analysis.

2.2 Material Models

The simulated soil volume consists of 10 node tetrahedral elements, and the behavior of sandy soil considered in the study is simulated using the Hardening Soil material model. The raft component is modeled considering a plate element which is a 6 node

triangular element, and the modeling of the pile component is considered with the help of an embedded beam element with a special interface element. Both raft and pile behavior is considered as linear-elastic. The interaction between the soil and the structural components is considered with the help of 12 node interface elements. The reduced shear strength at the soil-structure interface is taken into account by the Interface Reduction Factor (R_{int}).

For the present study, the soil properties of the homogeneous dense sand are considered from Nguyen et al. [5] and are shown in Table 1. Both the raft and piles are considered to be concrete material having a modulus of elasticity equal to 30,000 MPa with Poisson's ratio of 0.15.

Table 1. Input parameters for Plaxis 3D.

Soil Properties	**Dense Sand**
Relative density (%)	85
Dry unit weight, γ_d (kN/m^3)	15.6
Secant Young's modulus , E_{50}^{ref} (MPa)	37.67
Oedometer stiffness, E_{oed}^{ref} (MPa)	37.67
Unloading/reloading stiffness, E_{ur}^{ref} (MPa)	115.2
Friction angle, ϕ (°)	43
Cohesion , c (kPa)	0
Poisson's ratio, υ	0.25
Dilatancy angle, ψ(°)	11
Raft and Pile Properties	
Modulus of elasticity, E (MPa)	30,000
Poisson's ratio, υ	0.15
Unit weight, γ (kN/m^3)	25

2.3 Model Validation

The numerical model used for the present study is validated with that of centrifuge test results performed by Park and Lee [1] by modeling the foundation on a prototype scale with a centrifuge acceleration of 60 g. The piled-raft foundation of a 9 × 9 m raft having a thickness 1.2 m and 4 × 4 pile configuration with spacing of pile 2.4 m and a pile of 0.6 m diameter and 15 m length are considered. Silica sand with 84% relative density having an elastic modulus of 50 MPa and friction angle of 41° has been used for the analyses. The results of the load-settlement curve for piled-raft foundation obtained from both numerical study and centrifuge test are compared and shown in Fig. 3. The centrifuge test result appears to predict a bit higher stiffness value; however, the overall response shows a reasonably close match with a similar trend of the load-settlement

curve. This validated numerical model is then further used to carry out the numerical analysis for the present study.

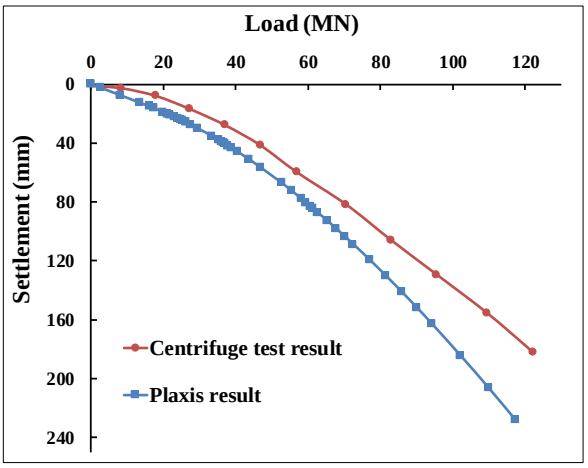

Fig. 3. Validation of the numerical model with the result of centrifuge test.

3 Results and Discussions

The evaluation of the load-sharing ratio of a large PR foundation in dense sand with respect to average settlement by varying parameters like pile spacing and length and raft thickness has been carried out. Initially, the individual load-settlement responses of the raft and piles in PR are determined for all the considered PR configurations which are compared with the individual responses of the unpiled raft and group piles, respectively. A large piled-raft foundation of 5 × 5 pile configuration with a raft of size (25 × 25) m, with raft thickness varied as 0.7 m, 2.0 m, and 4.7 m corresponding to relative raft-soil stiffness ratio (K_{rs}) of 0.4, 10, and 117 respectively [5], and piles of diameter 1 m are considered. The pile spacing and length are normalized with respect to pile diameter. The pile spacing is varied as s/d ratio of 2.5, 3, 4, and 5, while the pile length is varied as L/d ratio of 10, 15, 20, and 25. These various parameters of the structural elements considered for the study are also shown in Table 2. The uniformly distributed load of 600 kPa is applied on the foundation. The average settlement (W_{avg}) is calculated by considering the center settlement (W_{center}) and the corner settlement (W_{corner}) of the raft and is calculated by Eq. 1 [6]. The proportion of raft and pile load share is measured by the load-sharing ratio (α_{PR}), which is defined as the ratio of load carried by the piles in PR to the total applied load on the foundation.

$$W_{\text{avg}} = \frac{1}{3}(2W_{\text{center}} + W_{\text{corner}}) \quad (1)$$

3.1 Individual Load-Settlement Responses of Raft and Piles in PR

The load-settlement response of PR represents the combined load-settlement responses of both the raft as well as the piles, and therefore, it can be decomposed into the individual components as the raft in PR and piles in PR. The load taken by piles in PR (P_{PR}) is obtained by adding the axial loads from the individual pile heads, and the load taken by raft in PR (R_{PR}) is determined by subtracting the load taken by P_{PR} from the total applied load on the foundation. The individual load vs. W_{avg} responses of the R_{PR} and P_{PR} are plotted for different foundation configurations, and comparisons are made with those of unpiled raft (UR) and group piles (GP) as shown in Figs. 4 to 8.

Table 2. Raft and pile parameters considered for the present study.

Raft Parameters	**Values**
Raft width, B_r (m)	25 × 25
Raft thickness, t_r (m)	0.7*, 2.0, 4.7
Relative raft-soil stiffness ratio, K_{rs}	0.4*, 10, 117
Pile Parameters	
Pile number	5 × 5
Pile diameter, d (m)	1
Pile spacing to diameter ratio, s/d	2.5, 3, 4, 5
Pile length to diameter ratio, L/d	10, 15, 20, 25*

*standard value if not varied

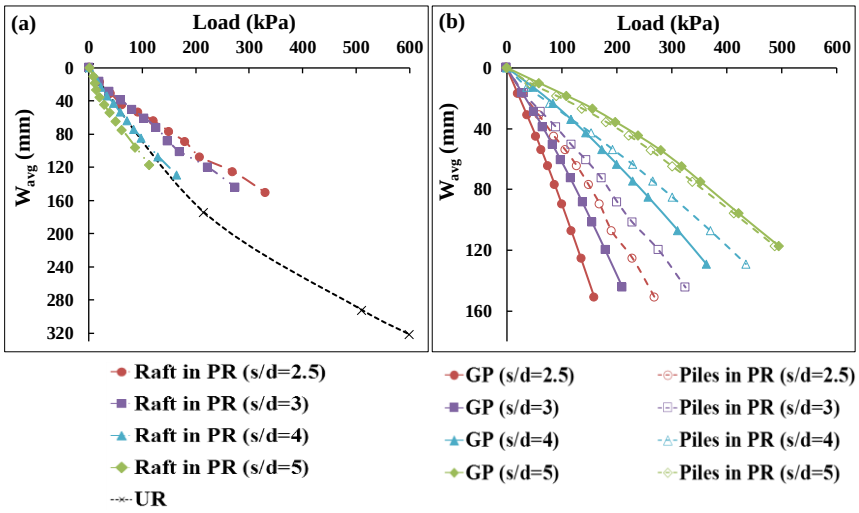

Fig. 4. Individual load vs. W_{avg} responses of (a) raft in PR compared with unpiled raft and (b) piles in PR compared with group piles for different pile spacing.

Fig. 4 shows the individual load vs. W_{avg} responses of the raft in PR and piles in PR compared with UR and GP for different pile spacings, respectively. From Fig. 4(a), it can be seen that as compared to UR, the load vs. W_{avg} response of R_{PR} is higher for smaller pile spacing (s/d ratios of 2.5 and 3) (indicating higher load carrying capacity) whereas for s/d ratio of 5, the load vs. W_{avg} response of R_{PR} is lesser than that of UR. It is observed that as the pile spacing increases, the load-carrying capacity of R_{PR} decreases, which means that the proportion of load carried by the piles becomes higher. From Fig. 4(b), the load vs. W_{avg} response of P_{PR} is higher when compared to group piles for all pile spacing except for s/d ratio of 5, where the load vs. W_{avg} response of P_{PR} is slightly lesser than that of GP. As the pile spacing increases, the proportion of load carried by the P_{PR} increases.

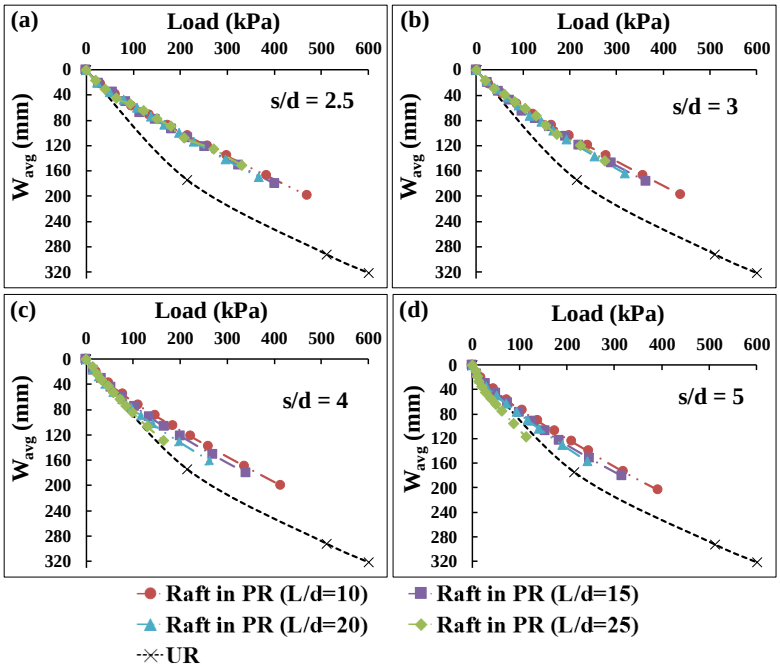

Fig. 5. Individual load vs. W_{avg} responses of raft in PR compared with unpiled raft for different pile lengths.

Fig. 5 shows the individual load vs. W_{avg} responses of R_{PR} compared with UR for different pile lengths at various pile spacings. For all pile spacing, it is observed that the load vs. W_{avg} response of R_{PR} is higher than UR for all the considered pile lengths (except for the L/d ratio of 25 at the s/d ratio of 5). As the pile length increases, there is no significant change in the load vs. W_{avg} response of R_{PR} in the case of s/d ratio of 2.5 and 3; however, the load carrying capacity decreases for pile spacing of s/d ratio of 4 and 5. The reason for the decrease in the load-carrying capacity of R_{PR} when the pile length is increased at larger pile spacing is that there is reduced overlapping of the stress and displacement fields between the piles leading to increased mobilization of pile capacity, which increases as the pile length increases.

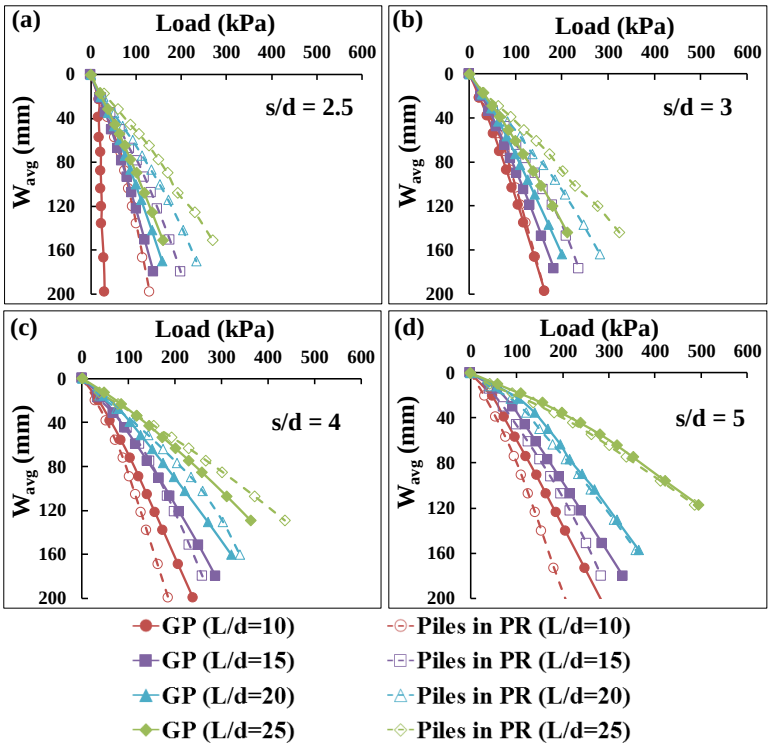

Fig. 6. Individual load vs. W_{avg} responses of piles in PR compared with group piles for different pile lengths.

Fig. 6 shows the individual load vs. W_{avg} responses of P_{PR} compared with group piles for different pile lengths at various pile spacings. From Figs. 6(a) and (b), at *s*/*d* ratio of 2.5 and 3, it is observed that the load vs. W_{avg} response of P_{PR} is higher than group piles for all the considered pile lengths. From Fig. 6(c), at *s*/*d* ratio of 4, it is noticed that the load vs. W_{avg} response of P_{PR} is lower than group piles for pile length of *L*/*d* ratio 10 and 15 but for *L*/*d* ratio of 20 and 25, the load vs. W_{avg} response of P_{PR} is still higher than group piles. From Fig. 6(d), at pile spacing of *s*/*d* ratio of 5, the load vs. W_{avg} response of P_{PR} is significantly lower than group piles for *L*/*d* ratio of 10 and 15 while it is slightly lower for the pile lengths of *L*/*d* ratio 20 and 25. For all *s*/*d* ratios, as the pile length increases (from *L*/*d* ratio of 10 to 25), the load carried by the piles increases, which is found to be more significant for *s*/*d* ratio of 4 and 5.

Fig. 7 shows the individual load vs. W_{avg} responses of R_{PR} compared with UR for different raft thicknesses at various pile spacings. From Figs. 7(a) and (b), at *s*/*d* ratio of 2.5 and 3, it is observed that the load vs. W_{avg} response of R_{PR} is higher than URs for all raft thicknesses. As the raft thickness increases, the load carried by R_{PR} decreases. For *s*/*d* ratio of 4 and 5 (Figs. 7(c) and (d)), the load vs. W_{avg} response of R_{PR} becomes almost equal to that of UR for all raft thicknesses except for raft thickness of 0.7 m (at s/d ratio of 5) where the load vs. W_{avg} response of R_{PR} becomes less than that of UR. As the raft thickness increases, there is no significant change in the load carried by R_{PR} for *s*/*d* ratio of 4; however, for *s*/*d* ratio of 5, the load carried by R_{PR} starts increasing as the

raft thickness increases. Fig. 8 shows the individual load vs. W_{avg} responses of P_{PR} compared with GP for different raft thicknesses at various pile spacings. From Figs. 8(a) and (b), at s/d ratio of 2.5 and 3, the load vs. W_{avg} response of P_{PR} is lower than GP for all raft thicknesses (except for t_r = 0.7 m). With increasing thickness of raft from 0.7 m to 2 m, the load carried by P_{PR} increases but then starts decreasing when the raft thickness is increased further up to 4.7 m. For s/d ratio 5 (Figs. 8(d)), the load vs. W_{avg} response of P_{PR} also becomes almost equal to that of GP for raft thickness of 0.7 m. As the raft thickness increases, the load carried by P_{PR} starts to decrease.

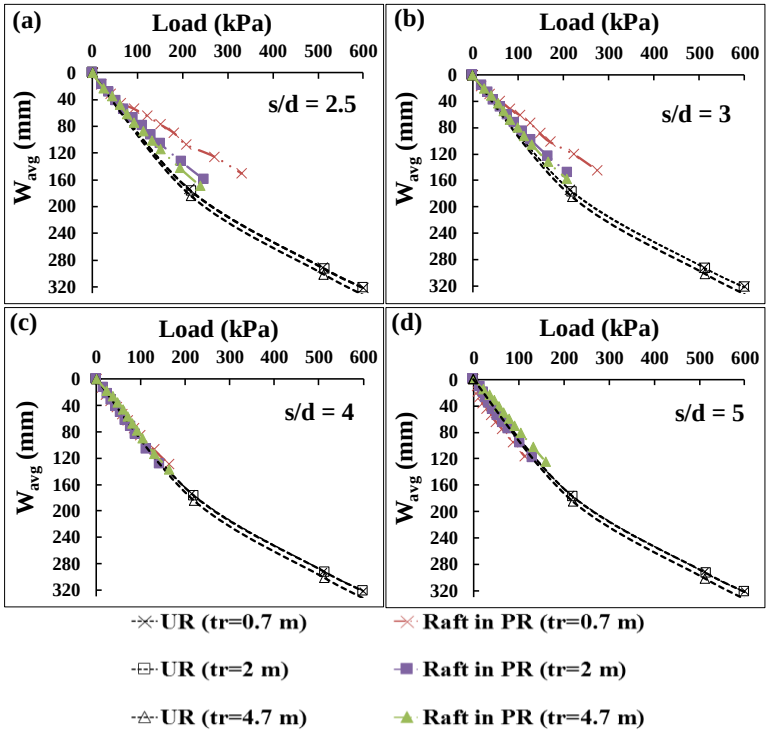

Fig. 7. Individual load vs. W_{avg} responses of raft in PR compared with unpiled raft for different raft thicknesses.

3.2 Variation of Load-Sharing Ratio with Settlement

In this section, the evaluation of load-sharing ratio of a large PR foundation in dense sand with respect to average settlement by varying pile spacing and length, and raft thickness has been discussed. Fig. 9 shows the variation of α_{PR} with W_{avg} for different pile spacings. With increasing pile spacing, the α_{PR} value increases at all settlement levels. For pile spacing of s/d ratio 2.5 and 3, the α_{PR} value decreases with W_{avg} because the piles are not able to properly mobilize their skin friction at lower pile spacing. For s/d ratio of 4 and 5, the α_{PR} value increases initially at initial settlement and then starts decreasing towards higher settlement because at higher settlement, the pile skin friction got fully mobilized and raft capacity starts to mobilize hence, the α_{PR} value starts decreasing towards higher settlement.

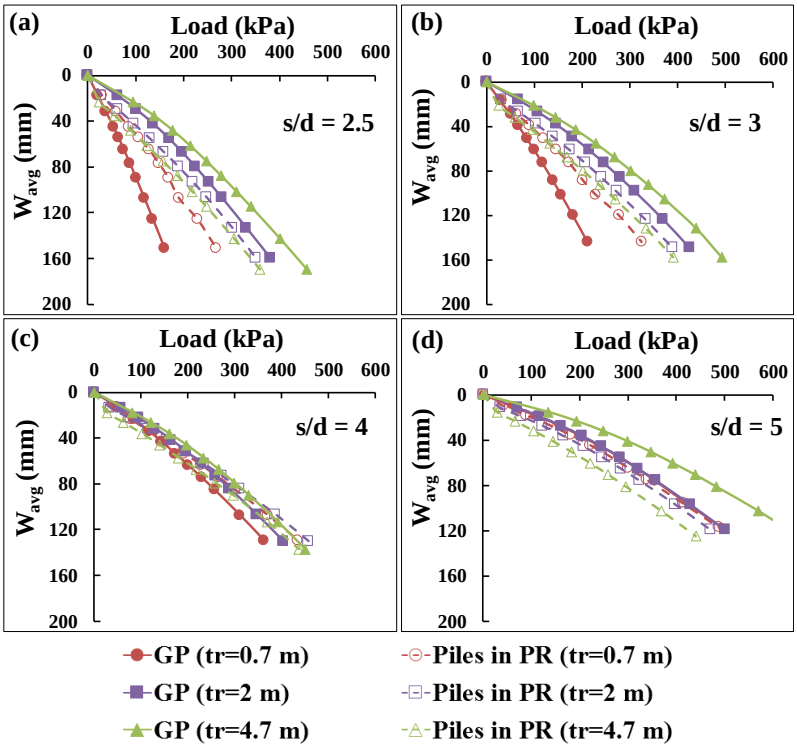

Fig. 8. Individual load vs. W_{avg} responses of piles in PR compared with group piles for different raft thicknesses.

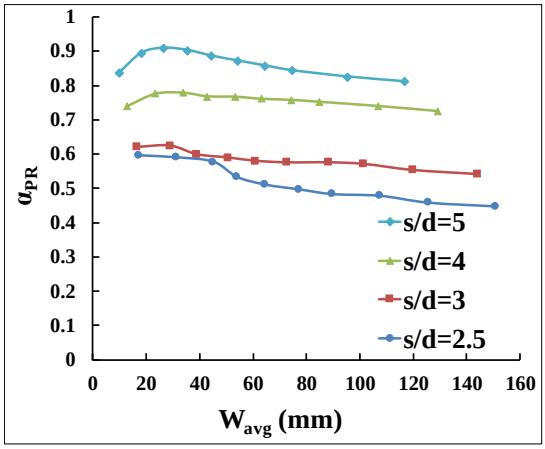

Fig. 9. Variation of load-sharing ratio with W_{avg} for different pile spacings.

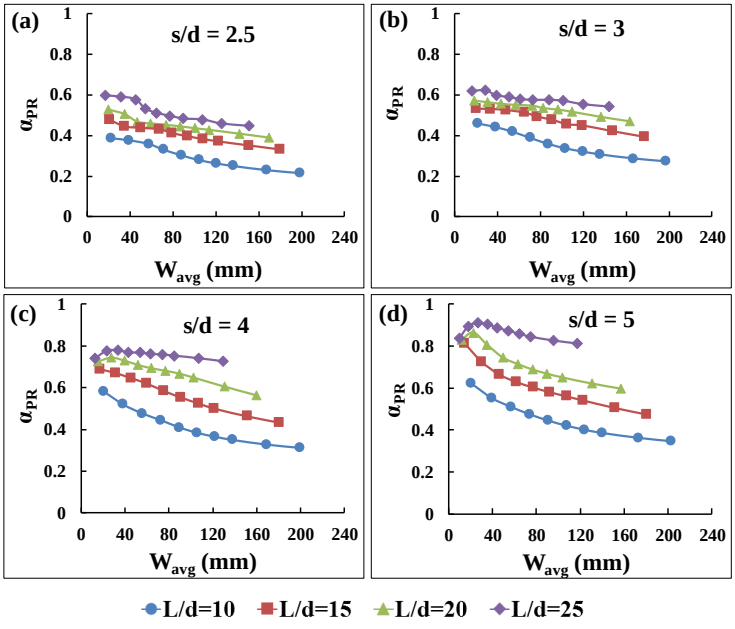

Fig. 10. Variation of load-sharing ratio with W_{avg} for different pile lengths at various pile spacings.

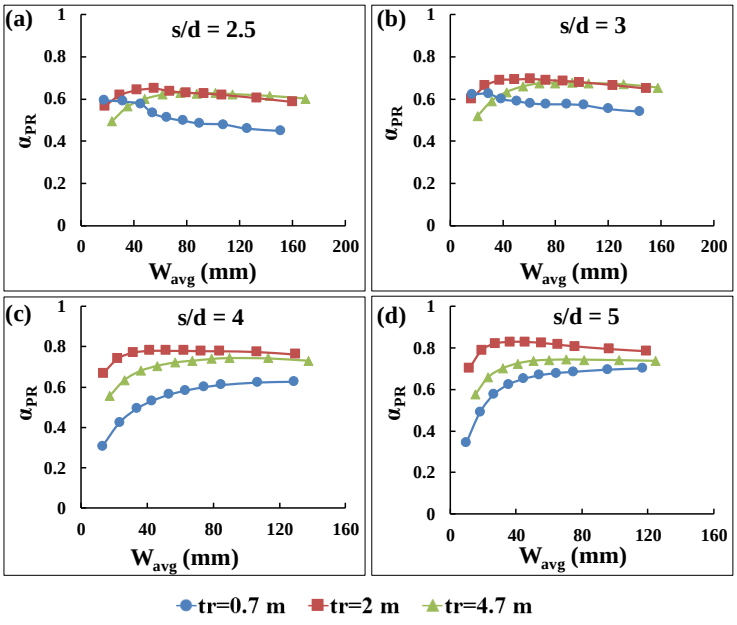

Fig. 11. Variation of load-sharing ratio with W_{avg} for different raft thicknesses at various pile spacings.

Fig. 10 shows the variation of α_{PR} with W_{avg} for different pile lengths at various pile spacings. It is observed that for *s*/*d* ratio of 2.5 and 3, the α_{PR} value kept decreasing with increasing settlement for all pile lengths; however, for *s*/*d* ratio of 4 and 5, the α_{PR} value increases at initial settlement range then decreases towards higher settlement for longer pile lengths of *L*/*d* ratios 20 and 25. As the pile length increases, the α_{PR} value increases at all settlement levels which is more significant in case of *s*/*d* ratio of 4 and 5 as compared to *s*/*d* ratio of 2.5 and 3. Fig. 11 shows the variation of α_{PR} with W_{avg} for different raft thicknesses at various pile spacings. As the raft thickness increases, the α_{PR} value increases (for *s*/*d* ratio of 4 and 5) which is significant at initial settlement. The load sharing ratio increases as the W_{avg} increases and becomes almost constant towards higher settlement for all raft thicknesses (Figs. 11(c) and (d)).

4 Conclusions

The settlement based load-sharing ratio variation for large piled-rafts on dense sand has been investigated through numerical modeling by varying parameters such as pile spacing, pile length, and raft thickness. From the comparison of the individual load vs W_{avg} response of raft and piles in PR with UR and GP respectively, the raft and piles in PR show higher load-carrying capacity than that of UR and GP, respectively, for the PR foundation configuration with raft thickness of 0.7 m, having a smaller pile spacing and longer pile lengths. For the *s*/*d* ratio of 2.5 and 3, the α_{PR} value decreases with $W_{avg,}$ whereas for the *s*/*d* ratio of 4 and 5, the α_{PR} value increases initially at initial settlement and then starts decreasing towards higher settlement. It was observed that the α_{PR} value kept decreasing with increasing W_{avg} for all pile lengths (*s*/*d* ratio of 2.5 and 3); however, the α_{PR} value increased at the initial settlement range and then decreased towards a higher settlement for longer pile lengths (*L*/*d* ratio of 20 and 25) for *s*/*d* ratio of 4 and 5. As the raft thickness increases, the α_{PR} value increases (for *s*/*d* ratio of 4 and 5), which is significant at initial settlement.

References

1. Park, D., & Lee, J.: Comparative analysis of various interaction effects for piled rafts in sands using centrifuge tests. Journal of Geotechnical and Geoenvironmental Engineering 141(1), 040140821-10 (2015).
2. Lee, J., Park, D., Park, D., & Park, K.: Estimation of load-sharing ratios for piled rafts in sands that includes interaction effects. Computers and Geotechnics 63, 306-314 (2015).
3. Viggiani, C., Mandolini, A., Russo, G.: Piles and Pile Foundation. 1st edn. Spon Press, London & New York (2012).
4. Brinkgreve, R., Swolfs, W., & Engin, E.: PLAXIS user's manual, version 6.1. Balkema, Rotterdam, The Netherlands (2015).
5. Nguyen, D. D. C., Jo, S. B., & Kim, D. S.: Design method of piled-raft foundations under vertical load considering interaction effects. Computers and Geotechnics 47, 16-27 (2013).
6. Reul, O., & Randolph, M. F.: Design strategies for piled rafts subjected to non uniform vertical loading. Journal of Geotechnical and Geoenvironmental Engineering 130(1), 1-13. (2004).